Virology 538 (2019) 86–96

Contents lists available at ScienceDirect

Virology

journal homepage: www.elsevier.com/locate/virology

Inferring host roles in bayesian phylodynamics of global avian influenza A virus H9N2

Jing Yang[a,b,c], Dong Xie[b,c], Zhen Nie[a], Bing Xu[a,d,*], Alexei J. Drummond[b,c]

[a] State Key Laboratory of Remote Sensing Science, College of Global Change and Earth System Science, Beijing Normal University, Beijing, China
[b] School of Computer Science, University of Auckland, Auckland, New Zealand
[c] Centre for Computational Evolution, University of Auckland, Auckland, New Zealand
[d] Department of Earth System Science, Tsinghua University, Beijing, China

ARTICLE INFO

Keywords:
Avian influenza virus
H9N2
Phylogeographic
Phylodynamic
Bayesian
Avian host transitions
Generalized linear model
Poultry trade

ABSTRACT

Role of avian hosts in shaping persistence, evolution, and dispersal of global low pathogenic avian influenza virus (LPAIV) H9N2 remains uncertain. Under Bayesian Markov Chain Monte Carlo framework, we used the discrete trait analysis (DTA) to reconstruct host and location switches in the evolutionary history of global H9N2 given hemagglutinin gene sequences from 18 countries/regions between 1976 and 2018. We employed generalized linear models (GLMs) to inform virus migration rates by empirical predictors. Global H9N2 isolates were mostly sampled from domestic Phasianidae in low- and middle-income countries with poor bio-security. Anatidae was inferred as the ancestral source from which the virus spread to domestic waterfowl, and later to domestic Phasianidae who have become the dominant host to sustain the virus, especially in Asia. Poultry trade was a well-supported driver to H9N2 spread across countries/regions. Strict bio-security and separation between wild and domestic poultry can be used to mitigate virus spread.

1. Introduction

Outbreaks of avian influenza virus (AIV) H9N2 can cause great economic losses for the poultry sector by reducing egg production and rates of weight gain (Zhang et al., 1994; Chen et al., 1994; Kim et al., 2006). The virus has been isolated in multiple species of both domestic and free-living birds worldwide. The first H9N2 isolate was collected from a turkey in Wisconsin state, the United States in 1966 (Homme and Easterday, 1970) and then the virus was mostly detected from shorebirds and wild ducks in North America (Kawaoka et al., 1988; Sharp et al., 1993). In Asia, the first recorded virus isolate was from the domestic duck in Hong Kong in 1978. In the late 1990s, the virus had spread to multiple Asian countries and become endemic in domestic poultry in some of them (Banks et al., 2000; Guan et al., 1999; Cameron et al., 2000; Nili and Asasi, 2003). Active surveillance on AIVs in Europe initially identified very low circulation of H9N2 subtype, but its prevalence in wild waterfowl increased in recent years (Baumer et al., 2010; Lindh et al., 2014; Munster et al., 2007). In Africa, firstly recorded H9N2 virus occurred in ostriches in South Africa in 1995 (Alexander, 2000); at the end of 2010, the virus was detected in Egypt where it became endemic in poultry and co-circulated with high pathogenic avian influenza virus (HPAIV) H5N1 (Kandeil et al., 2014; Kim, 1003). In South America, the first H9N2 was isolated from a wild aquatic bird in Argentina in 2007 and it is genetically related to the virus in North America (Xu et al., 2012); more H9N2 isolates were sampled in aquatic birds later. Increasing geographic extent of H9N2 AIVs in birds poses a threat to global poultry production, marketing industry, and wildlife health.

Based on the phylogenetic relationship and antigenic divergence, the phylogeny of global H9N2 HA genes can be broadly grouped into the Eurasian lineage and the North American lineage. The Eurasian lineage can be further clustered into three sublineages: the G1-like sublineage (represented by A/quail/Hong Kong/G1/97), the G9-like sublineage (or Y280-like sublineage; represented by A/chicken/Hong Kong/G9/97 or A/duck/Hong Kong/Y280/97 or A/chicken/Beijing/1/94) and the Korea lineage (or Y439-like lineage; represented by A/chicken/Korea/38349-p96323/96 or A/duck/Hong Kong/Y439/97) (Guo et al., 2000). The G1-like viruses mainly circulate in the Middle East and southern Asia, whereas other two sublineages predominantly include isolates from eastern and southeastern Asia (Shahsavandi et al., 2012; Shanmuganatham et al., 2016; Davidson et al., 2013). In addition, the internal genes of H9N2 also showed great genetic diversity and

* Corresponding author. Department of Earth System Science, Tsinghua University, Beijing, China.
E-mail addresses: jingauckland2017@gmail.com (J. Yang), bing.xu2013@gmail.com (B. Xu).

https://doi.org/10.1016/j.virol.2019.09.011
Received 2 July 2019; Received in revised form 24 September 2019; Accepted 24 September 2019
Available online 27 September 2019

multiple genotypes defined by the phylogenetic divergence of all eight genes continued to emerge (Cui et al., 2014; Sun et al., 2010; Li et al., 2017). In an attempt to control and eradicate H9N2 in poultry, inactivated vaccines were employed in mainland China, Pakistan, Iran, Israel, and South Korea (Li et al., 2017; Davidson et al., 2013; Lee and Song, 2013; Naeem and Siddique, 2006). However, these extensive vaccination programs did not eliminate poultry infections and the vaccinated chicken can still carry and transmit the virus (Pu et al., 2015).

H9N2 virus can directly infect human from poultry (Peiris et al., 1999) as a zoonotic pathogen. Since the first human case caused by H9N2 was reported in 1999 in Hong Kong (Peiris et al., 1999), human infections sporadically occurred in mainland China, Hong Kong, Bangladesh, and Egypt (https://www.who.int/influenza/human_animal_interface/avian_influenza/archive/en/). Confirmed human cases increased in mainland China from 2013 to 2017 and often had exposure to poultry or their contaminated fomites before disease onset (Li et al., 2017). Further, some H9N2 AIVs possess a Q226L amino-acid replacement that gives rise to a human-like receptor specificity of the hemagglutinin (HA) gene (Sun and Liu, 2015; Kim, 1003). Recently increasing isolations of this variant in poultry from Asia further facilitate the virus adaption to humans in the future (Wan and Perez, 2007). As influenza is a multi-segmented virus, reassortment can occur when a host is infected with multiple influenza strains. Gene segment exchanges can give rise to novel genotypes with altered phenotypic characteristics affecting viral replication, transmission, or pathogenicity (Sun et al., 2010; Xu et al., 2007). Several such reassortment events involving H9N2 viruses have been uncovered by genetic analyses (Pu et al., 2015; Guan et al., 1999). The G1-like H9N2 virus donated its internal genes to HPAIV H5N1, which caused both human and poultry infections in Hong Kong in 1997 (Guan et al., 1999). In addition, the genotype G57 of H9N2 shared its internal gene segments with the novel H7N9 and H10N8 AIVs that caused human infections in 2013 in China (Pu et al., 2015; Qi et al., Liu). Cocirculation of H9N2 and other influenza subtypes (e.g. H5N1 and H7N3 in the Middle East) in poultry increases the risk of human exposure and human infection with H9N2 or with novel zoonotic influenza subtypes generated by acquiring genetic materials from H9N2 (Kim, 1003).

Avian acts as a major host to sustain the prevalence and dispersal of avian influenza A virus (Baele et al., 2015; Bahl et al., 2016). Poultry trade network connects poultry farms and markets, and it may help to explain the spatial dissemination of global H9N2. The G1-like H9N2 viruses are dominantly prevalent in middle eastern and southern Asian countries and these isolates share a common ancestor with the virus from Hong Kong (Shanmuganatham et al., 2014, 2016; Fusaro et al., 2011). Genetically related H9N2 in separated locations suggests a potential role of poultry trade in virus spread (Shanmuganatham et al., 2014). High-density setting coinciding with complex avian species and spatial sources during the process of poultry trade can provide an ideal environment for interspecies virus transmission and gene reassortment (Choi et al., 2005). In addition, the rapid spread of HPAIV H5N1 from Asia to Europe and Africa in 2005–2006 suggested that migratory bird can be a major candidate for long-distance diffusion of influenza virus (Olsen et al., 2006). The potential of migratory wildfowl contributing to H5N1 dissemination has been confirmed by both large-scale satellite telemetry and phylodynamic analysis given genetic data (Gaidet et al., 1147; Baele et al., 2015). Further, ecosystem interactions of domestic and wild birds can also contribute to global influenza transmission; domestic poultry is considered as a major driver of regional virus spread while wild birds typically drive a long-distance dispersal of influenza (Bahl et al., 2016).

The discrete trait analysis (DTA) model is a commonly used Bayesian phylogeographic method to infer the migration history of sampled lineages given genetic data. The DTA models the migration of lineages between different traits as the DNA substitution process using a continuous-time Markov model (Lemey et al., 2009). This approach improves computational efficiency by integrating over all possible migration histories when computing phylogenetic likelihoods efficiently by a pruning algorithm (Felsenstein, 1981). Further, DTA model helped to reconstruct the migration patterns of H9N2 within China and between regions (Jin et al., 2014; Wei and Li, 2018), to elucidate the role of long-distance migratory birds in the global spread of H5N8 (for H5N8 and Viruses, 2016), and to disentangle the contribution of different avian hosts to shape the complex disease ecology of H5N1 (Baele et al., 2015). In addition, DTA model can be augmented with a generalized linear model (GLM) parameterization of migration rates in order to use time-stamped viral genetic sequence data to uncover potential explanatory factors (Lemey et al., 2014). This integration of DTA and GLM can simultaneously reconstruct transmission history between different hosts and estimate the contribution of underlying predictors to cross-species transmission of rabies virus (Faria et al., 2013).

In our study, we elucidate the contributions of different avian hosts and their interactions to the persistence, evolutionary dynamics, and dispersal of global H9N2. First, we described spatial distribution and temporal dynamic of global H9N2 isolates sampled from avians. Further, we inferred migration dynamics of host and location states in the evolutionary process of global H9N2 AIVs using DTA model under a Bayesian Markov chain Monte Carlo (MCMC) inference framework, given HA gene sequences isolated in 18 countries/region in the year 1976-2018. We also estimated the Markov jumps and rewards of host traits to clarify the contribution of each avian host to global H9N2 persistence and circulation. Subsequently, we used GLM models to parameterize estimated migration rates of H9N2 viruses by a series of underlying predictors, e.g. poultry trade, poultry production, geographic distance, and climatic data.

2. Materials and methods

2.1. Genetic data

Avian influenza H9N2 is not a notifiable animal disease that required to report to the World Organisation for Animal Health (OIE). In our study, we examined the spatiotemporal pattern of global H9N2 isolates sampled from birds based on their HA nucleotide sequences recorded in the GenBank Influenza Virus Database (http://www.ncbi.nlm.nih.gov/genomes/FLU/FLU.html) hosted by the National Center for Biotechnology Information (NCBI). We obtained the description information of avian-origin H9N2 HA nucleotide sequences in the year 1966–2018 (downloaded on March 1st, 2019). We excluded sequences lacking date, country/region, or host information. We kept one of the identical sequences caused by duplicated submissions. Further, we divided virus hosts into two avian families, Anatidae (including ducks, geese, and swans), Phasianidae (including chickens, quails and pheasants), one avian superorder, Neoaves (such as pigeons, sparrows and falcons), and unknown avian host (including ratites and birds without species details) (Baele et al., 2015). We geocoded and pooled above description about H9N2 HA sequences into groups according to their countries/regions, host types, and collection years.

We also downloaded nucleotide sequences of these H9N2 HA genes with a minimum of 90% full-length between 1966 and 2018. To avoid potentially phylodynamic inference bias caused by extremely few isolates in some locations, we removed sequences in locations with less than 10 isolates between 1966 and 2018. We aligned sequences by default parameters in MAFFT v7 (Katoh and Standley, 2013). We removed outliers identified in the molecular clock test in TempEst (Rambaut et al., 2016). To reduce spatial heterogeneity and improve computational efficiency, we downsampled our virus sequences. We employed two downsampling strategies to investigate the impact of heterogeneous sampling intensity across locations on our analyses. We obtained two data sets including 686 and 1037 sequences by randomly sampling at most 5 and 10 isolates per country/region per year respectively. In both data sets, sequences were isolated between 1976 to

June 14th, 2018 from 18 countries/regions, including Algeria, Bangladesh, Hong Kong (China), mainland China (described as China hereafter), Egypt, India, Indonesia, Iran, Israel, Japan, Jordan, the Netherlands, Pakistan, South Korea, Uganda, United Arab Emirates, the USA, and Vietnam. We demonstrate phylodynamic inferences given 686 sequences here, and results inferred by 1037 sequences are shown in the supplement. Details on virus sequences are also provided in supplementary materials (Figs. S1–S2 and Table S2).

2.2. Empirical predictors

According to previous researches and practical considerations, we chose multiple underlying predictors to inform H9N2 spread across 18 locations (Lemey et al., 2014; Dudas et al., 2017; Müller et al., 2018). Predictor selection and data sources are described in our previous research (Yang et al., 2019). The predictors we investigated include poultry trade, poultry production, gross domestic product values (GDP), geographic distance, a predictor describing if two countries/regions share a border on the continent, temperature, temperature seasonality, rainfall, rainfall seasonality, relative humidity, and virus isolate quantity. All predictors are available on country/region level between 1976 and 2018, except the poultry trade data are obtained between 1986 and 2013, and the poultry production data are accessible between 1976 and 2017. We filled missing values with the data in the nearest year. We tested collinearity of predictors and excluded the GDP, rainfall and rainfall seasonality for the Pearson correlation coefficients between them and predictor temperature exceed 0.65. Further, we calculated the logarithm of the predictors and standardized them with a mean of 0 and a standard deviation of 1, excepting the binary predictor. This is standard practice to eliminate the effect of the magnitude of different predictors when using GLMs to inform viral migration rates (Lemey et al., 2014; Faria et al., 2013).

2.3. Spatiotemporal visualizations

Given the information about the location and host sources of global H9N2 HA genes between 1966 and 2018, we projected the spatial distribution and host constitution of global H9N2 isolates to a world map on country/region level in QGIS v2.18 (http://qgis.osgeo.org). Further, we visualized temporal dynamics of global H9N2 isolates as well as location and host changes using the incidence package in R v3.4.3 (Kamvar et al., 1000; Jombart et al., 2019).

2.4. Parameter inferences

Under Bayesian MCMC framework, we performed discrete phylogeographic inferences to construct geographic dispersal and host transitions in the evolutionary history of H9N2 AIVs by DTA in BEAST v1.10.4 (Suchard et al., 2018). We employed an HKY nucleotide substitution model with gamma site model which has 4 rate categories, a strict clock, and the Bayesian skyline tree prior to model sequence evolution and trait changes. We used an asymmetric discrete trait substitution model and its integrated Bayesian stochastic search variable selection procedure (BSSVS) to estimate transition rates between traits (Lemey et al., 2009). Exploratory analyses with an alternative uncorrelated lognormal relaxed clock model show consistent phylogeographic inferences (data not shown). We also inferred all transitions between host states and the time spent in hosts between two transitions by calculating Markov jumps and Markov rewards respectively. Further, we used multiple empirical predictors to inform the H9N2 migration rates between locations in DTA GLMs. We performed at least 3 parallel runs for each phylodynamic analysis with 50 or 100 million MCMC lengths to get converged and mixed parameter estimates. We removed an appropriate burn-in (10%–25% of samples in most cases) to achieve an adequate effective sample size (ESS, >200) of parameter estimates in Tracer v1.7 (Rambaut et al., 2018). We got the maximum clade credibility (MCC) tree from the posterior phylogenetic trees in TreeAnnotator. We visualized and annotated the time-scaled phylogenetic trees with the maximum probable location and host on the branch respectively by FigTree v1.4.3 (http://tree.bio.ed.ac.uk/software/figtree/) and the ggtree package in R v3.4.3 (Yu et al., 2017). The xml files of Bayesian phylodynamic inferences and R codes of visualization are available at https://github.com/judyssister/globalH9N2Host.git.

2.5. Generalized linear models

The GLM as an extension of DTA can inform H9N2 dispersal across countries/regions by a series of underlying factors. It describes virus migration rates as a linear combination of coefficients, indicators, and predictors in a log-space as equations (1) and (2). In both equations, m_{ij} represents the virus migration rate from location i and j, and $i \neq j$; $p_{k\{ij\}}$ represents the kth predictor between region i and j; I_k and β_k represent the indicator and coefficient of the kth predictor respectively. The indicator describes if the predictor is included in the model and the coefficient describes the effect size of each predictor contributing to migration rates. In equation (2), we include an additional error term α to explain the variance of migration rates that cannot be completely elucidated by the predictors. We set the prior inclusion probability of no predictor included in a GLM as 50% and the prior probability of each predictor inclusion equals. In addition, we also tested the impact of virus sampling heterogeneity across locations by considering the number of viral isolates as a distinctive predictor in both equations. We investigated four migration rate GLMs in this study.

$$\log m_{ij} = \sum_{k=1}^{n} (I_k \beta_k \log p_{k\{ij\}}) \quad (1)$$

$$\log m_{ij} = \sum_{k=1}^{n} (I_k \beta_k \log p_{k\{ij\}}) + \alpha \quad (2)$$

3. Results

3.1. Spatial distribution of H9N2 isolates

Between 1966 and 2018, H9N2 AIVs have been widely isolated from birds in countries/regions in Asia, Europe, Africa, and the Americas (Fig. 1). Most H9N2 isolates were collected from domestic poultry and from countries in Asia, Europe, and northern Africa. The largest H9N2 isolates were found in Asia, especially in mainland China with approximately 63% of global H9N2 isolates between 1994 and 2018. Further, host constitution of H9N2 isolates was divergent across continents. In Asia and northern Africa, the H9N2 isolates were largely collected from Phasianidae, especially the domestic chicken. But Anatidae was the primary host of H9N2 isolates in Europe and the Americas. Interestingly, H9N2 sampling isolates can be negatively associated with the economic level of corresponding country/region, which is supported by a Wilcoxon rank-sum test especially in Asia and Europe. More isolates were collected in the low- and middle-income countries and mainly from Phasianidae. However, in the high-income countries, relatively few H9N2 isolates were found and they mostly came from Anatidae.

3.2. Temporal pattern of H9N2 isolates and effective population sizes

Analyses on location and host sources of global H9N2 isolates revealed that the isolates were mainly hosted by Anatidae in regions with higher latitudes while mostly hosted by Phasianidae in lower latitude regions (Figs. 1 and 2). Before the mid-1990s, H9N2 was isolated in fewer countries and often from a singular host (e.g. Anatidae or Phasianidae) in each location (Fig. 2). Since the 1990s, H9N2 began to be

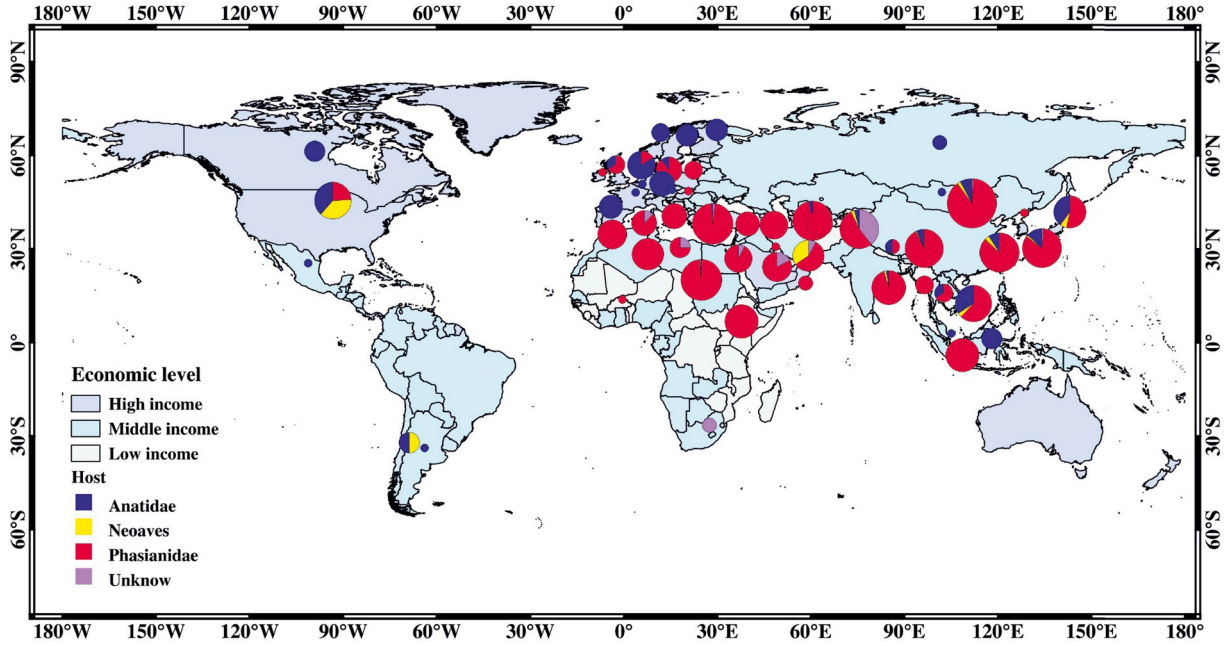

Fig. 1. Spatial distribution of global avian influenza H9N2 isolates between 1966 and 2018. Diameter of circle is positively related to virus isolate quantity in each country/region. Colors in the circle indicate the fraction of viral host origins (see legend). Fill color of each country/region represents its economic condition. The source of world borders dataset with economic development information is the Natural Earth Data (https://www.naturalearthdata.com/).

isolated in multiple countries, especially in Asian countries, and viral host sources became more diverse in each location. Of note, H9N2 virus was consistently isolated in the Phasianidae in mainland China and Iran since its first emergence. In addition, both the number of H9N2 isolates and viral effective population size showed an increasing trend with a slight decrease in the most recent years (Fig. 3). H9N2 isolates from mainland China accounted for a large portion of global isolates. Since 1995, more isolates were collected from Phasianidae in comparison with these from Anatidae and Neoaves annually.

3.3. Hosts contributing to virus transition and persistence

Anatidae is the inferred ancestral host of global H9N2 viruses (posterior probability (*pp*) is 81%, Fig. 4a). Initially H9N2 virus persisted in Anatidae from which the virus spread to Phasianidae later. In the USA, the virus jumped back to Anatidae from the Phasianidae since the late 1990s. In many infected countries of Asia, H9N2 largely persisted in Phasianidae and sporadic spillovers spread from Phasianidae to Anatidae or Neoaves. Anatidae was a dominant host to sustain virus evolution in Europe. Further, H9N2 viruses circulating in Phasianidae from South Korea, in the wild Anatidae from the Netherlands and Japan, and in the wild Neoaves from the USA have close genetic relationships.

Both the Bayesian inferred transition rates and Markov jumps across hosts of H9N2 show that viral host transition from Phasianidae to Anatidae is the most frequent, and following from Anatidae to Phasianidae, from Phasianidae to Neoaves, from Anatidae to Neoaves, with strong supports (Fig. 4 and Table 1). The transition frequency from Neoaves to other hosts is the lowest. In addition, the estimates of Markov reward time in hosts showed that H9N2 spent more time persisting in Phasianidae; the following is in Anatidae, and the time of H9N2 virus staying in Neoaves is the shortest. Further, the inferences on virus diffusion rates can be affected by the heterogeneous samples across hosts. Especially sparsity of sampling from Neoaves can result in weak conclusions on its contribution to H9N2 spread.

3.4. Geographic dispersal of H9N2 viruses

We estimated location state changes in the evolutionary history of global H9N2 viruses in the year 1976–2018 by the Bayesian phylodynamic inference. The global H9N2 phylogeny supports previously established lineages – the American lineage and the Eurasian lineage; the Eurasian lineage can be further divided into three sublineages: G9-like, G1-like, and the Korea sublineage (Fig. 4b). Isolates belonging to the American lineage were mostly collected from the USA. Majority of isolates within the G9-like sublineage were sampled from mainland China, Hong Kong, Vietnam, and Indonesia. In the G1-like sublineage, geographic sources of virus isolates are more complex, mainly including southern Asia (e.g. Indian, Bangladesh, and Pakistan), western Asia (including Iran, Isreal, Jordan, and the United Arab Emirates) and the African countries (Egypt, Algeria, and Uganda). Few isolates in the G1-like sublineage from Hong Kong and mainland China prior to the early 2000s. Further, isolates in the Korea sublineage were mainly sampled from South Korea, Japan, the Netherlands, and the northern USA. Within the Eurasian lineage, there is a small clade with H9N2 isolates from wild Anatidae of the USA.

Hong Kong was inferred as the geographic source ($pp = 88\%$) of H9N2 viruses (Fig. 4b). This ancestral root state was estimated given available genetic data and can be biased by the lack of samples from other locations in the 1970s and 1980s. Before 1970, H9N2 evolved into two groups and one part persistently circulated in the USA. The other part circulated in Hong Kong from where it spread to mainland China ($pp = 62\%$), to countries in southern and western Asia ($pp = 42\%$), and to South Korea and the Netherlands ($pp = 36\%$) respectively; the latter two migration events from Hong Kong are uncertain with low posterior probabilities. Frequent migration events occurred between countries in southern Asia and the Middle East, and the following occurred in eastern and southeastern Asia.

In addition, virus migration rates we inferred were highest between mainland China and Hong Kong, and followings were from mainland China to Japan, from Pakistan to Iran, from Isreal to Jordan, from Japan to the Netherlands, from Pakistan to the United Arab Emirates, from Hong Kong to Vietnam, from Vietnam to Japan, from India to Bangladesh, from the United Arab Emirates to Isreal, and from Jordan

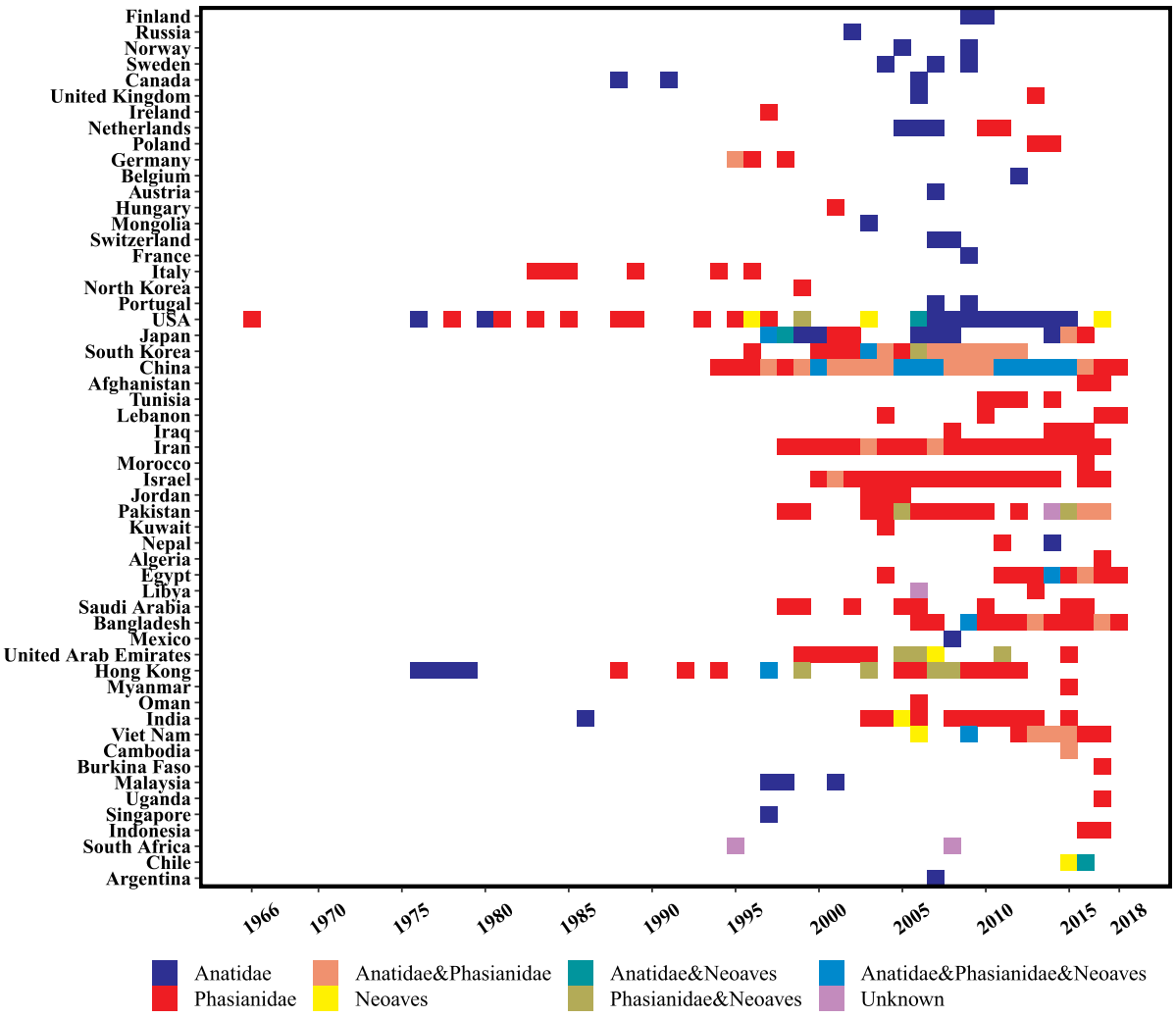

Fig. 2. Temporal dynamics of host sources of global H9N2 isolates from 1966 to 2018. Countries/regions are listed according to their central latitudes. Here, Finland is the northernmost country and Argentina is the southernmost country. Color of each square indicates the host origins of H9N2 isolates (see legend).

to Isreal in a descending order, with strong supports (Fig. 5). Further, these estimated migration rates between each pair of locations are larger than 1, which means more than one migration event occurs between locations in a year. Many of the well-supported diffusion pathways together with high migration rates occur between locations that are in relative proximity-.

3.5. Underlying predictors to virus spread

We used several underlying predictors to inform the migration rates of H9N2 viruses among 18 countries/regions by four DTA GLMs under Bayesian phylogeographic framework. According to the posterior and prior probability (qp) of predictor inclusion in a GLM, we evaluated the support of each predictor by a Bayes Factor (BF; $BF = (pp/(1-pp))/(qp/(1-qp))$) (Suchard et al., 2001). A BF over 3 and 20 indicates suggestive and strong support of a predictor being included in the model respectively (Suchard et al., 2001). In four migration rate GLMs, predictors including poultry trade, sharing a border, and temperature at the destination location were identified as strongly supported (Fig. 6). We inferred poultry trade positively contributed to virus migration rates. A higher migration rate can exist between locations sharing a border on the continent. Further, the temperature at the destination location was negatively related to virus migration. In addition, including virus isolate quantity in each location as separated predictors and adding an error term have a negligible impact on the interpretation of the results from the GLMs.

4. Discussion

In this study, we investigated the role of different avian hosts in persistence, evolution and spatial dispersal of global H9N2 influenza A viruses by Bayesian phylodynamic inferences. In addition, we integrated empirical predictors and genetic data to explore the underlying mechanism contributing to virus spread between countries/regions by DTA GLMs.

4.1. Host constitution of global H9N2 isolates

The sampling size and host constitution of global H9N2 isolates seem to be related to latitudes and economic conditions of the infected countries/regions. In the low- and middle-income countries with lower latitudes, large H9N2 isolates were collected from Phasianidae. In the high-income countries with higher latitudes, few H9N2 isolates were found and mostly from Anatidae. Further, the Phasianidae isolates we used are mostly from domestic poultry, and the Anatidae isolates include samples from both domestic and wild birds. We investigated the difference of poultry density among the infected countries/regions, and this difference cannot explain the latitude-dependent divergence of

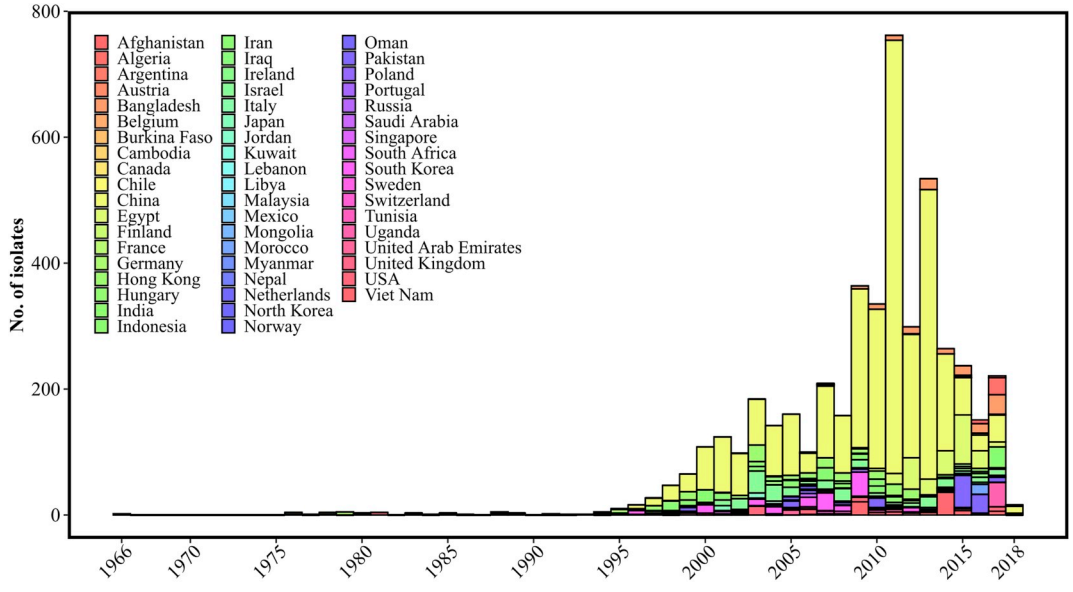

(a) Temporal pattern with locations.

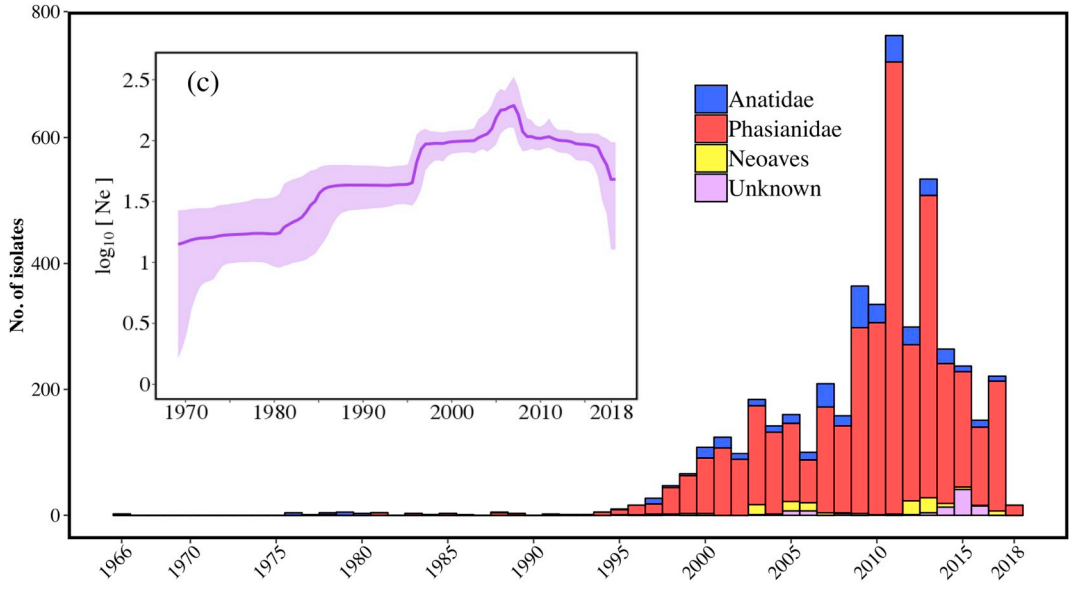

(b) Temporal pattern with hosts.

Fig. 3. Temporal dynamics of isolates and effective population size of global H9N2 from 1966 to 2018. Temporal patterns of H9N2 isolates (a) with location and (b) with host information. Figure (c) shows the Bayesian skyline of effective population size of global H9N2.

viral host sources (http://www.fao.org/ag/againfo/programmes/documents/livatl2/poultry_density.htm). A Wilcoxon rank-sum test supports that the divergent virus-host constitutions are associated with the economic level of the corresponding countries/regions especially in Asia and Europe. Poor bio-security condition and confused management practices in live poultry markets and farms can facilitate virus prevalence and divergence in the low- and middle-income countries, especially in Asia (Gao, 2014). High investments into bio-sanitation of poultry practice and trade system in the high-income countries can mitigate the persistence and transmission of H9N2 viruses in domestic poultry, though infections in wild birds are usually hard to eliminate.

4.2. Host roles in virus persistence and spread

Our Bayesian-based phylogeny of global H9N2 supports previously documented virus lineages (Guo et al., 2000). Novel virus isolates continuously emerged in these established lineages, with better fitness to specific locations and avian hosts (Pu et al., 2015; Shanmuganatham et al., 2014). Further, genetically divergent H9N2 viruses persisted in wild Anatidae. Genetic similarity between H9N2 isolates from wild Anatidae in the USA and from the Eurasian lineage indicated the intercontinental gene exchanges contributed by migratory birds, especially in their Arctic breeding sites (Björn Olsen et al., 2006). Further, Anatidae and Hong Kong were inferred as the ancestral sources of H9N2 given the limited genetic data we used. In the mid-1980s, Anatidae can

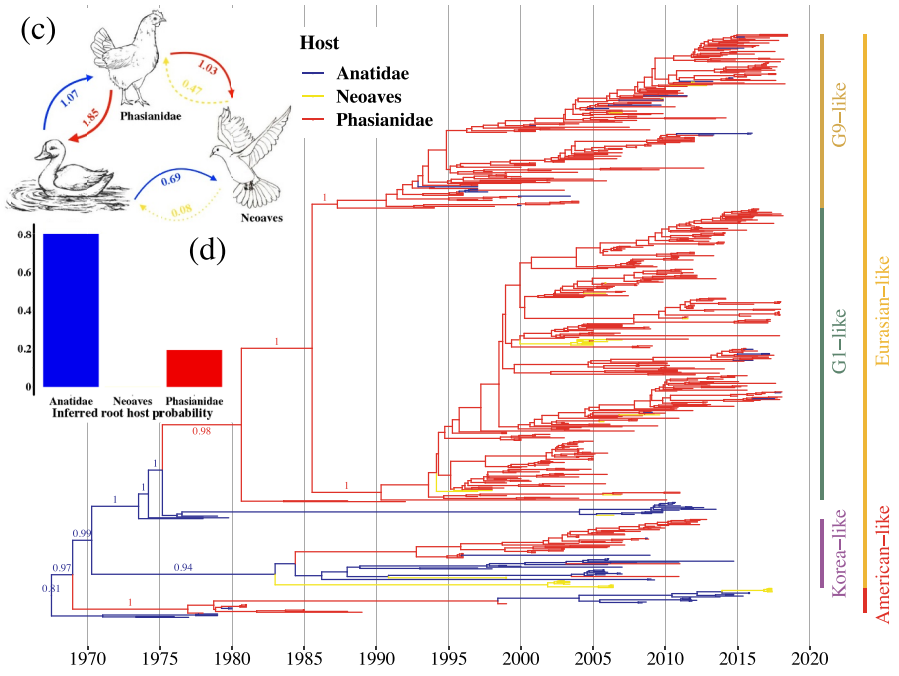

(a) With host transitions.

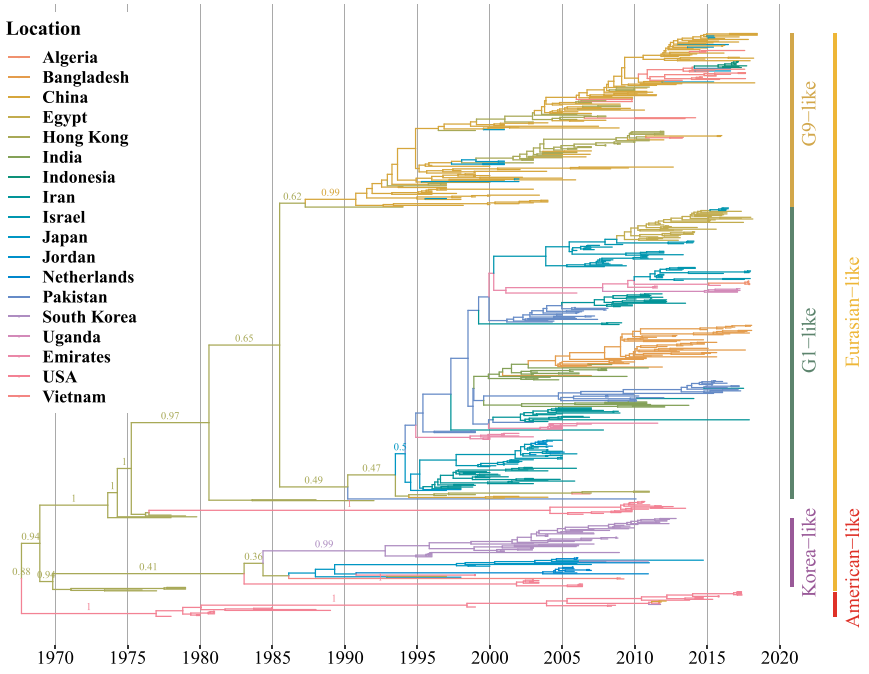

(b) With location transitions.

Fig. 4. Time-scaled phylogenetic trees of global H9N2 influenza viruses. (a) With inferred hosts and (b) with estimated locations on the branches. Colours of tree branches indicate hosts or locations with the maximum probability (see legend). A colour change on a branch indicates a host transition or a location migration event. Numbers on branches represent posterior probability of displayed host or location. H9N2 originated from the Anatidae and Hong Kong from where it spread to East Asia and West and South Asia respectively. H9N2 can originally spread from its natural reservoir to free-ranging domestic waterfowl, later spreading to domestic Phasianidae, and Phasianidae became the dominant host to sustain the virus. (c) shows mean transition rates across hosts, and solid, dashed and dotted line represents rate with strong, suggestive and no support respectively. (d) shows posterior probabilities of ancestral hosts. Bars on the right indicate the established lineages, and phylogenetic cluster of isolates from the neighbouring regions indicates easier virus interactions in close proximity.

play a role in the H9N2 spread from Hong Kong to South Korea and Europe. Before the early 1990s, the movement of Phasianidae contributed to the virus spread from Hong Kong to mainland China and to other countries in western Asia (Shanmuganatham et al., 2014). Of note, the low posterior probability (<50%) supports transition routes from Hong Kong to other locations. These uncertain migration events can result from the lack of virus isolates before 1995 (Fig. 3). In addition, domestic Phasianidae played a key role in the persistence and dispersal of H9N2 viruses in southeastern, eastern, southern, western Asia and northern Africa. Wild Anatidae dominantly contributed to the circulation and transition of H9N2 viruses in the USA and the Netherlands.

Since Anatidae isolates we investigated include samples from both domestic and wild birds, we propose that H9N2 can originally spread from its natural host wild waterfowl to the free-ranging domestic waterfowl by contacts. Hereafter, the H9N2 in Hong Kong spread from

Table 1
Asymmetric mean estimates on Markov host jumps and reward time of H9N2 virus.

	Jumps			Rewards (years)
	Anatidae	Neoaves	Phasianidae	
Anatidae	–	3.91 (3, 5)	6.52 (5, 9)	338.93 (307.98, 367.75)
Neoaves	0.02 (0, 0)	–	1.37 (0, 3)	46.55 (30.91, 63.03)
Phasianidae	25.79 (24, 28)	14.12 (13, 16)	–	1606.48 (1557.47, 1656.67)

Note: values in bracks represent 95% HPD intervals.

domestic waterfowl to domestic Phasianidae, and later the virus evolved to be adaptable to Phasianidae with efficient replication and transmission. We also find that global H9N2 viruses spent a much longer time in Phasianidae than that in Anatidae and Neoaves. We suggest that Phasianidae has already become the dominant host to sustain the persistence and circulation of global H9N2 viruses, especially the domestic chicken. To meet the increasing demand for animal protein, global chicken production increased, with a huge population and rapid growth in recent years (http://faostat.fao.org). Further, chicken can provide a fitting environment for the existence and evolution of H9N2 AIVs in Asia (Pu et al., 2015), and the virus could silently sustain and evolve in the infected chicken population without showing clinical symptoms (Sun and Liu, 2015). In addition, the genetically related relationship between Phasianidae and Anatidae facilitates the interspecies transmission of H9N2 between them with comparison to other pairs of avian hosts (https://en.wikipedia.org/wiki/Fowl). We speculate that sporadic virus isolates in Anatidae and Neoaves recently are spillovers from domestic Phasianidae, and they could not persist in Anatidae and Neoaves for the host-specific virus adaption. Cutdown contacts between wild birds and free-ranging domestic poultry and separation of different avian species in poultry farms can be effective measures to mitigate cross-species transmission and spatial dispersal of H9N2.

The phylodynamic analyses and ancestral state reconstructions were restricted to available H9N2 samples (Bahl et al., 2016). Especially prior to 1990s, the lack of samples can bias the ancestral state estimation of global H9N2. Systematic and long-term surveillance programs on H9N2 AIVs can provide more information to construct a thorough phylodynamics of the virus. Additionally, data granularity in time, space and host can have a decisive effect on our hypothesis testing and model construction. High-resolution data can allow us to test more refined hypotheses, to model influenza movements in a smaller geographic region, and to better understand the role of avian species in influenza virus ecology and evolution (Lindh et al., 2014; Xu et al., 2007).

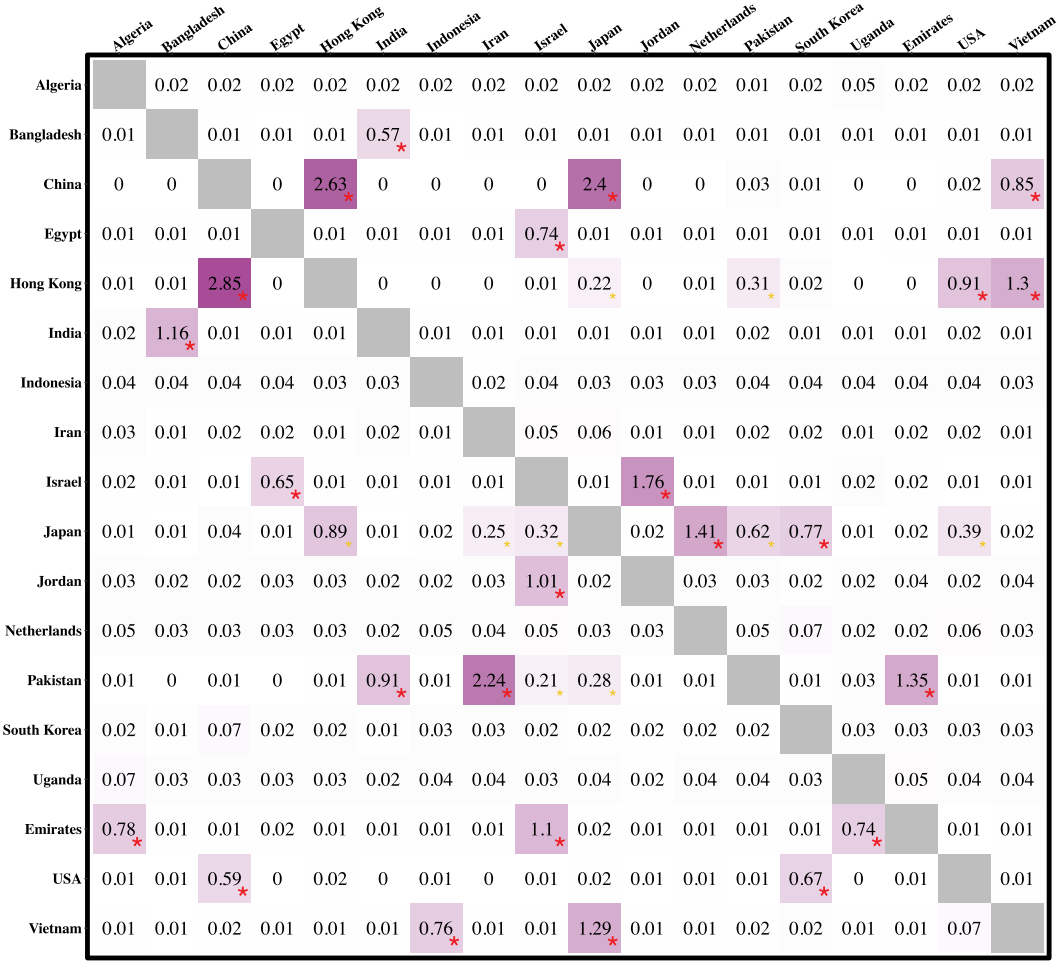

Fig. 5. Asymmetric migration rate matrix of H9N2 between countries/regions. Unit is the number of migration events per lineage per year. The y-axis represents the original locations and the x-axis represents the destinations. The background color of the cell indicates the magnitude of migration rates; the dark purple corresponds to a higher rate, while the white color corresponds to a lower rate. Bayes factors of migration rates over 3 and 20 are labelled by a yellow and a red asterisk in the cell respectively. The large and well-supported rates are occurred between locations in proximity, suggesting some underlying factors related to geographic distance contribute to virus spread.

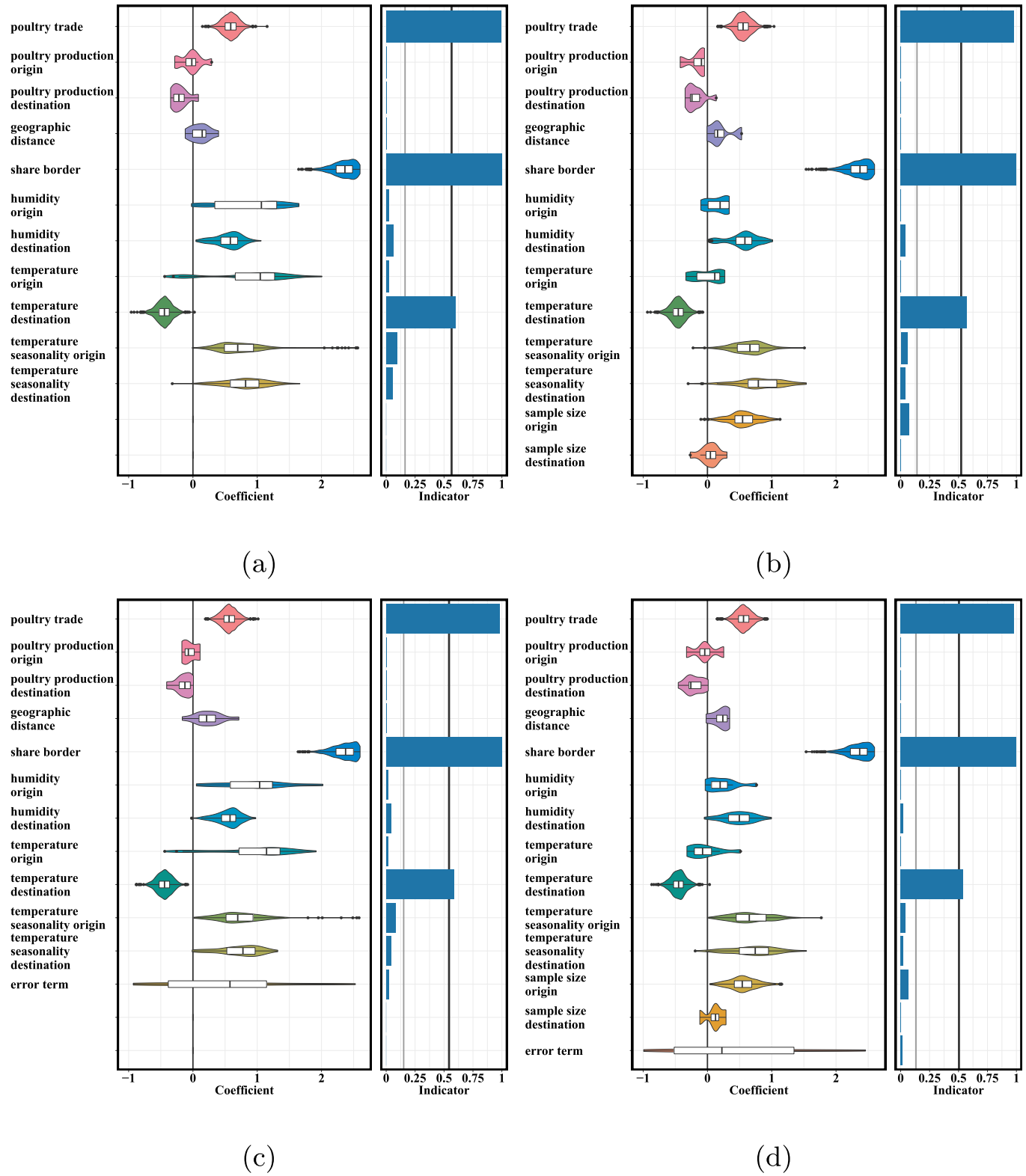

Fig. 6. Predictors of migration rates of global H9N2 between countries/regions. The estimated coefficients and inclusion probabilities for potential predictors of migration rates in DTA models: (a), (b) without and (c), (d) with adding an error term in the GLMs; (a), (c) without and (b), (d) with including isolate quantity as distinctive predictors. Prior probability of no predictors being included in a GLM is 50%. Coefficient shows the effect size of predictor contributing to H9N2 migration rates when the predictor was included in the GLM. Inclusion probability represents the proportion of a predictor included in the GLM in all posterior samples. Bayes factor 3 and 20 are labelled by a thin and thick vertical line in the indicator plot respectively. Predictors poultry trade, sharing a border, and temperature in destination are strongly supported factors to inform virus spread in all GLMs. Error terms have a negligible effect on the results from GLMs.

4.3. International live poultry trade drives virus spread

International live poultry trade can facilitate global H9N2 dispersal with strong support in DTA GLMs we investigated. Asymptomatic poultry can be ignored during poultry trade and transportation, and the movement of sick poultry increases the risk of virus spreading to a "naive" poultry flock and to a new location. Further, the illegal trade of poultry or captive birds in the border regions of countries also contribute to the virus spread across countries. Previous DTA GLM analysis failed to identify the contribution of poultry trade to H9N2 spread among geographic regions for the potential estimation bias caused by duplicated predictors included in the GLM (e.g. predictor poultry import and poultry export) (Wei and Li, 2018). Also, we find that a higher virus migration rate could occur between countries/regions who share a border on the continent. In addition to the poultry trade with low freight costs between nearby countries, the mobile wild birds can also carry the virus to a new country from its proximity. We also find the lower temperature in destination contributes to virus migrations, and the longer survival of influenza viruses at lower temperature possibly explains this contribution.

Heterogeneous virus sampling across locations can enlarge the uncertainty of migration rate estimates between each pair of locations under DTA model, since such a model assumes that the sample size is proportional to virus population size in each location (De Maio et al., 2015; Lemey et al., 2009). In the present study, we repeated our phylodynamic inferences under two sampling scenarios, and our reconstructions and inferences on global H9N2 are robust to potential sampling intensity bias across locations in DTA (Figs. S3–S4 and Table S1). Further, the well-supported predictors that driving H9N2 diffusion are consistent in all migration rate GLMs we estimated (Fig. S5). Including a random effect as an extra predictor in GLMs does not change our results and their statistical supports. Our results are consistent and robust in spite of variations in sample sizes and with respect to the empirical predictors considered in DTA.

5. Conclusion

In our study, we find that quantity and host constitution of global H9N2 isolates are related to the economic level of the infected countries/regions. The bio-security and management should be improved in poultry farms and markets to reduce virus prevalence in domestic Phasianidae and in the low- and middle-income countries. Our Bayesian phylodynamic inferences provided further evidence to support that Anatidae can be an ancestral source of global H9N2 and the virus can spread from its natural reservoir wild waterfowl to the free-ranging domestic waterfowl, and later spreading to domestic Phasianidae. Currently, domestic Phasianidae has become the dominant host to sustain virus persistence, evolution, and dispersal, especially in Asia. Migratory Anatidae can help the sporadically transcontinental gene exchanges of H9N2. In addition, international live poultry trade can drive the global spread of H9N2 avian influenza, especially between nearby countries sharing a border on the continent. Strict quarantine on poultry import can mitigate the virus spread by poultry trade.

Declarations of interest

None.

Acknowledgment

We would like to thank Guangchuang Yu and Jun Cai for their help in plotting. We also would like to thank the New Zealand eScience Infrastructure (NeSI) for their supply of high-performance computing facilities. Thanks a lot to China Scholarship Council (CSC) for the financial support to Jing Yang to visit Centre of Computational Evolution in the University of Auckland, New Zealand to carry out this work. Fundings have been provided by the National Research Program of the Ministry of Science and Technology of the People's Republic of China (2016YFA0600104), and donations from Delos Living LLC and the Cyrus Tang Foundation to Tsinghua University.

Appendix A. Supplementary data

Supplementary data to this article can be found online at https://doi.org/10.1016/j.virol.2019.09.011.

References

Alexander, D.J., 2000. A review of avian influenza in different bird species. Vet. Microbiol. 74 (1), 3–13. https://doi.org/10.1016/S0378-1135(00)00160-7 http://www.sciencedirect.com/science/article/pii/S0378113500001607.

Baele, G., Lemey, P., Trovão, N.S., Suchard, M.A., Gilbert, M., 2015. Bayesian inference reveals host-specific contributions to the epidemic expansion of influenza a H5N1. Mol. Biol. Evol. 32 (12), 3264–3275. https://doi.org/10.1093/molbev/msv185. arXiv. http://oup.prod.sis.lan/mbe/article-pdf/32/12/3264/17472195/msv185.pdf.

Bahl, J., Pham, T.T., Hill, N.J., Hussein, I.T.M., Ma, E.J., Easterday, B.C., Halpin, R.A., Stockwell, T.B., Wentworth, D.E., Kayali, G., Krauss, S., Schultz-Cherry, S., Webster, R.G., Webby, R.J., Swartz, M.D., Smith, G.J.D., Runstadler, J.A., 2016. Ecosystem interactions underlie the spread of avian influenza a viruses with pandemic potential. PLoS Pathog. 12 (5), 1–20. https://doi.org/10.1371/journal.ppat.1005620.

Banks, J., Speidel, E.C., Harris, P.A., Alexander, D.J., 2000. Phylogenetic analysis of influenza a viruses of h9 haemagglutinin subtype. Avian Pathol. 29 (4), 353–359. https://doi.org/10.1080/03079450050118485. pMID: 19184825. arXiv. https://doi.org/10.1080/03079450050118485. https://doi.org/10.1080/03079450050118485.

Baumer, A., Feldmann, J., Renzullo, S., Müller, M., Thuer, B., Hofmann, M., 2010. Epidemiology of avian influenza virus in wild birds in Switzerland between 2006 and 2009. Avian Dis. 54 2, 875–884.

Cameron, K., Gregory, V., Banks, J., Brown, I., Alexander, D., Hay, A., Lin, Y., 2000. H9n2 subtype influenza a viruses in poultry in Pakistan are closely related to the h9n2 viruses responsible for human infection in Hong Kong. Virology 278 (1), 36–41. https://doi.org/10.1006/viro.2000.0585.

Chen, B., Zhang, Z., Chen, W., 1994. The study of avian influenza: Ithe isolation and preliminary serological identification of avian influenza virus in chicken. Chin. J. Vet. Med. 20, 3–5.

Choi, Y.K., Seo, S.H., Kim, J.A., Webby, R.J., Webster, R.G., 2005. Avian influenza viruses in Korean live poultry markets and their pathogenic potential. Virol. 332 (2), 529–537. https://doi.org/10.1016/j.virol.2004.12.002 http://www.sciencedirect.com/science/article/pii/S0042682204008165.

Cui, L., Liu, D., Shi, W., Pan, J., Qi, X., Li, X., Guo, X., Zhou, M., Li, W., Li, J., Haywood, J., Xiao, H., Yu, X., Pu, X., Wu, Y., Yu, H., Zhao, K., Zhu, Y., Wu, B., Jin, T., Shi, Z., Tang, F., Zhu, F., Sun, Q., Wu, L., Yang, R., Yan, J., Lei, F., Zhu, B., Liu, W., Ma, J., Wang, H., Gao, G.F., 2014. Dynamic reassortments and genetic heterogeneity of the human-infecting influenza a (h7n9) virus. Nat. Commun. 5, 3142. EP –. https://doi.org/10.1038/ncomms4142.

Davidson, I., Shkoda, I., Golender, N., Perk, S., Lapin, K., Khinich, Y., Panshin, A., 2013. Genetic characterization of ha gene of low pathogenic h9n2 influenza viruses isolated in Israel during 2006–2012 periods. Virus Genes 46 (2), 255–263. https://doi.org/10.1007/s11262-012-0852-4.

De Maio, N., Wu, C.-H., OReilly, K.M., Wilson, D., 2015. New routes to phylogeography: a bayesian structured coalescent approximation. PLoS Genet. 11 (8), 1–22. https://doi.org/10.1371/journal.pgen.1005421.

Dudas, G., Carvalho, L.M., Bedford, T., Tatem, A.J., Baele, G., Faria, N.R., Park, D.J., Ladner, J.T., Arias, A., Asogun, D., Bielejec, F., Caddy, S.L., Cotten, M., D'Ambrozio, J., Dellicour, S., Di Caro, A., Diclaro, J.W., Duraffour, S., Elmore, M.J., Fakoli, L.S., Faye, O., Gilbert, M.L., Gevao, S.M., Gire, S., Gladden-Young, A., Gnirke, A., Goba, A., Grant, D.S., Haagmans, B.L., Hiscox, J.A., Jah, U., Kugelman, J.R., Liu, D., Lu, J., Malboeuf, C.M., Mate, S., Matthews, D.A., Matranga, C.B., Meredith, L.W., Qu, J., Quick, J., Pas, S.D., Phan, M.V.T., Pollakis, G., Reusken, C.B., Sanchez-Lockhart, M., Schaffner, S.F., Schieffelin, J.S., Sealfon, R.S., Simon-Loriere, E., Smits, S.L., Stoecker, K., Thorne, L., Tobin, E.A., Vandi, M.A., Watson, S.J., West, K., Whitmer, S., Wiley, M.R., Winnicki, S.M., Wohl, S., Wölfel, R., Yozwiak, N.L., Andersen, K.G., Blyden, S.O., Bolay, F., Carroll, M.W., Dahn, B., Diallo, B., Formenty, P., Fraser, C., Gao, G.F., Garry, R.F., Goodfellow, I., Günther, S., Happi, C.T., Holmes, E.C., Kargbo, B., Keïta, S., Kellam, P., Koopmans, M.P.G., Kuhn, J.H., Loman, N.J., Magassouba, N., Naidoo, D., Nichol, S.T., Nyenswah, T., Palacios, G., Pybus, O.G., Sabeti, P.C., Sall, A., Ströher, U., Wurie, I., Suchard, M.A., Lemey, P., Rambaut, A., 2017. Virus genomes reveal factors that spread and sustained the ebola epidemic. Nature 544, 309 (EP –).

Faria, N.R., Suchard, M.A., Rambaut, A., Streicker, D.G., Lemey, P., 2013. Simultaneously reconstructing viral cross-species transmission history and identifying the underlying constraints. Philos. Trans. R. Soc. Biol. Sci. 368 (1614), 20120196. https://doi.org/10.1098/rstb.2012.0196. arXiv. https://royalsocietypublishing.org/doi/pdf/10.1098/rstb.2012.0196.

Felsenstein, J., 1981. Evolutionary trees from dna sequences: a maximum likelihood approach. J. Mol. Evol. 17 (6), 368–376.

for H5N8, T.G.C., Viruses, R.I., 2016. Role for migratory wild birds in the global spread of avian influenza h5n8. Science 354 (6309), 213–217. https://doi.org/10.1126/

science.aaf8852. arXiv. https://science.sciencemag.org/content/354/6309/213.full.pdf.
Fusaro, A., Monne, I., Salviato, A., Valastro, V., Schivo, A., Amarin, N.M., Gonzalez, C., Ismail, M.M., Al-Ankari, A.-R., Al-Blowi, M.H., Khan, O.A., Maken Ali, A.S., Hedayati, A., Garcia Garcia, J., Ziay, G.M., Shoushtari, A., Al Qahtani, K.N., Capua, I., Holmes, E.C., Cattoli, G., 2011. Phylogeography and evolutionary history of reassortant h9n2 viruses with potential human health implications. J. Virol. 85 (16), 8413–8421. https://doi.org/10.1128/JVI.00219-11. arXiv. https://jvi.asm.org/content/85/16/8413.full.pdf. https://jvi.asm.org/content/85/16/8413.
Gaidet, N., Cappelle, J., Takekawa, J.Y., Prosser, D.J., Iverson, S.A., Douglas, D.C., Perry, W.M., Mundkur, T., Newman, S.H., 2010. Potential spread of highly pathogenic avian influenza h5n1 by wildfowl: dispersal ranges and rates determined from large-scale satellite telemetry. J. Appl. Ecol. 47 (5), 1147–1157. https://doi.org/10.1111/j.1365-2664.2010.01845.x. arXiv. https://besjournals.onlinelibrary.wiley.com/doi/pdf/10.1111/j.1365-2664.2010.01845.x.
Gao, G.F., 2014. Influenza and the live poultry trade. Sci. 344 (6181). https://doi.org/10.1126/science.1254664. 235–235. arXiv. http://science.sciencemag.org/content/344/6181/235.full.pdf. http://science.sciencemag.org/content/344/6181/235.
Guan, Y., Shortridge, K.F., Krauss, S., Webster, R.G., 1999. Molecular characterization of h9n2 influenza viruses: were they the donors of the “internal” genes of h5n1 viruses in Hong Kong? Proc. Natl. Acad. Sci. 96 (16), 9363–9367. https://doi.org/10.1073/pnas.96.16.9363. arXiv. http://www.pnas.org/content/96/16/9363.full.pdf.
Guo, Y., Krauss, S., Senne, D., Mo, I., Lo, K., Xiong, X., Norwood, M., Shortridge, K., Webster, R., Guan, Y., 2000. Characterization of the pathogenicity of members of the newly established h9n2 influenza virus lineages in asia. Virology 267 (2), 279–288. https://doi.org/10.1006/viro.1999.0115.
Homme, P.J., Easterday, B.C., 1970. Avian influenza virus infections. i. characteristics of influenza a/Turkey/wisconsin/1966 virus. Avian Dis. 14 (1), 66–74. http://www.jstor.org/stable/1588557.
Jin, Y., Yu, D., Ren, H., Yin, Z., Huang, Z., Hu, M., Li, B., Zhou, W., Yue, J., Liang, L., 2014. Phylogeography of avian influenza a h9n2 in China. In: BMC Genomics.
Jombart, T., Kamvar, Z.N., FitzJohn, R., Cai, J., Bhatia, S., Schumacher, J., Pulliam, J.R., 2019. Incidence: Compute, Handle, Plot and Model Incidence of Dated Events, R Package Version 1.7.0.
Z. N. Kamvar, J. Cai, J. R. Pulliam, J. Schumacher, T. Jombart, Epidemic curves made easy using the r package incidence [version 1; referees: awaiting peer review], F1000Res. 8 (139).
Kandeil, A.M., el Shesheny, R., Maatouq, A.M., Moatasim, Y., Shehata, M.M., Bagato, O., Rubrum, A.M., Shanmuganatham, K.K., Webby, R.R.J., Ali, M.I.A., Kayali, G., 2014. Genetic and antigenic evolution of h9n2 avian influenza viruses circulating in Egypt between 2011 and 2013. Arch. Virol. 159, 2861–2876.
Katoh, K., Standley, D.M., 2013. Mafft multiple sequence alignment software version 7: improvements in performance and usability. Mol. Biol. Evol. 30 (4), 772–780. https://doi.org/10.1093/molbev/mst010. arXiv. http://oup/backfile/content_public/journal/mbe/30/4/10.1093/molbev/mst010/3/mst010.pdf. https://doi.org/10.1093/molbev/mst010.
Kawaoka, Y., Chambers, T.M., Sladen, W.L., Gwebster, R., 1988. Is the gene pool of influenza viruses in shorebirds and gulls different from that in wild ducks? Virol. 163 (1), 247–250. https://doi.org/10.1016/0042-6822(88)90260-7 http://www.sciencedirect.com/science/article/pii/0042682288902607.
S.-H. Kim, Challenge for one health: Co-circulation of zoonotic h5n1 and h9n2 avian influenza viruses in Egypt, Viruses 10 (3). doi:10.3390/v10030121.
Kim, J.A., Cho, S.H., Kim, H.S., Seo, S.H., 2006. H9n2 influenza viruses isolated from poultry in Korean live bird markets continuously evolve and cause the severe clinical signs in layers. Vet. Microbiol. 118 (3), 169–176. https://doi.org/10.1016/j.vetmic.2006.07.007.
Lee, D.-H., Song, C.-S., 2013. H9n2 avian influenza virus in korea: evolution and vaccination. Clin. Exp.Vaccine Res. 2 (1), 26–33.
Lemey, P., Rambaut, A., Drummond, A.J., Suchard, M.A., 2009. Bayesian phylogeography finds its roots. In: PLoS Computational Biology.
Lemey, P., Rambaut, A., Bedford, T., Faria, N., Bielejec, F., Baele, G., Russell, C.A., Smith, D.J., Pybus, O.G., Brockmann, D., Suchard, M.A., 2014. Unifying viral genetics and human transportation data to predict the global transmission dynamics of human influenza h3n2. In: PLoS Pathogens.
Li, C., Wang, S., Bing, G., Carter, R.A., Wang, Z., Wang, J., Wang, C., Wang, L., Wu, G., Webster, R.G., Wang, Y., Sun, H., Sun, Y., Liu, J., Pu, J., 2017. Genetic evolution of influenza h9n2 viruses isolated from various hosts in China from 1994 to 2013. Emerg. Microb. Infect. 6 e106 EP. https://doi.org/10.1038/emi.2017.94.
Lindh, E., Ek-Kommonen, C., Väänänen, V.-M., Vaheri, A., Vapalahti, O., Huovilainen, A., 2014. Molecular epidemiology of h9n2 influenza viruses in northern europe. Vet. Microbiol. 172 (3), 548–554. https://doi.org/10.1016/j.vetmic.2014.06.020 http://www.sciencedirect.com/science/article/pii/S0378113514003125.
Müller, N.F.Dudas, G.Stadler, T. Inferring time-dependent migration and coalescence patterns from genetic sequence and predictor data in structured populations. bioRxivarXiv. https://www.biorxiv.org/content/early/2018/06/14/342329.full.pdf.
Munster, V.J., Baas, C., Lexmond, P., Waldenström, J., Wallensten, A., Fransson, T., Rimmelzwaan, G.F., Beyer, W.E.P., Schutten, M., Olsen, B., Osterhaus, A.D.M.E., Fouchier, R.A.M., 2007. Spatial, temporal, and species variation in prevalence of influenza a viruses in wild migratory birds. PLoS Pathog. 3 (5), 1–9. https://doi.org/10.1371/journal.ppat.0030061. https://doi.org/10.1371/journal.ppat.0030061.
Naeem, K., Siddique, N., 2006. Use of strategic vaccination for the control of avian influenza in Pakistan. Dev. Biologicals 124, 145–150.
Nili, H., Asasi, K., 2003. Avian influenza (h9n2) outbreak in Iran. Avian Dis. 47 (s3), 828–831. https://doi.org/10.1637/0005-2086-47.s3.828.
Olsen, B., Munster, V.J., Wallensten, A., Waldenström, J., Osterhaus, A.D., Fouchier, R.A., 2006. Global Patterns of Influenza A Virus in Wild Birds. Science 312, 384–388. https://doi.org/10.1126/science.1122438.
Olsen, B., Munster, V.J., Wallensten, A., Waldenström, J., Osterhaus, A.D.M.E., Fouchier, R.A.M., 2006. Global patterns of influenza a virus in wild birds. Science 312 (5772), 384–388. https://doi.org/10.1126/science.1122438. arXiv. https://science.sciencemag.org/content/312/5772/384.full.pdf.
Peiris, M.U., Yuen, K.Y., Leung, C.W., Chan, K.A., Ip, P.L.-S., Lai, R., Orr, W.K., Shortridge, K.F., 1999. Human infection with influenza h9n2. Lancet 354 9182, 916–917.
Pu, J., Wang, S., Yin, Y., Zhang, G., Carter, R.A., Wang, J., Xu, G., Sun, H., Wang, M., Wen, C., Wei, Y., Wang, D., Zhu, B., Lemmon, G., Jiao, Y., Duan, S.C., Wang, Q., Du, Q., Sun, M., Bao, J., Sun, Y., Zhao, J., Zhang, H., Wu, G., Liu, J., Webster, R., 2015. Evolution of the h9n2 influenza genotype that facilitated the genesis of the novel h7n9 virus. Proc. Natl. Acad. Sci. U.S.A. 112 2, 548–553.
W. Qi, X. K. Zhou, W. Shi, L. Huang, W. F. Xia, D. Liu, H. Li, S. L. Chen, F. Lei, L. Cao, J. Wu, F. He, W. Song, Q. Li, M. Liao, M. Liu, Genesis of the novel human-infecting influenza a(h10n8) virus and potential genetic diversity of the virus in poultry, China., Euro Surveill.: Bull. Eur. Maladies Transmissibles Eur. Commun. Dis. Bull. 19 25.
Rambaut, A., Lam, T.T., Carvalho, L.M., Pybus, O.G., 2016. Exploring the temporal structure of heterochronous sequences using tempest (formerly Path-O-Gen). 2 (1). https://app.dimensions.ai.on.2018/08/13 vew007, exported from.
Rambaut, A., Drummond, A.J., Xie, D., Baele, G., Suchard, M.A., 2018. Posterior summarisation in bayesian phylogenetics using tracer 1.7. Syst. Biol. https://doi.org/10.1093/sysbio/syy032. syy032arXiv. http://oup/backfile/content_public/journal/sysbio/pap/10.1093_sysbio_syy032/2/syy032.pdf. https://doi.org/10.1093/sysbio/syy032.
Shahsavandi, S., Salmanian, A.-H., Ghorashi, S.A., Masoudi, S., Ebrahimi, M.M., 2012. Evolutionary characterization of hemagglutinin gene of h9n2 influenza viruses isolated from asia. Res. Vet. Sci. 93 (1), 234–239. https://doi.org/10.1016/j.rvsc.2011.07.033.
Shanmuganatham, K., Feeroz, M.M., Jones-Engel, L., Walker, D., Alam, S., Hasan, M., McKenzie, P., Krauss, S., Webby, R.J., Webster, R.G., 2014. Genesis of avian influenza h9n2 in Bangladesh. Emerg. Microb. Infect. 3 (1), 1–17. https://doi.org/10.1038/emi.2014.84. arXiv. https://doi.org/10.1038/emi.2014.84.
Shanmuganatham, K.K., Jones, J.C., Marathe, B.M., Feeroz, M.M., Jones-Engel, L., Walker, D., Turner, J., Rabiul Alam, S.M., Kamrul Hasan, M., Akhtar, S., Seiler, P., McKenzie, P., Krauss, S., Webby, R.J., Webster, R.G., 2016. The replication of bangladeshi h9n2 avian influenza viruses carrying genes from h7n3 in mammals. Emerg. Microb. Infect. (4), e35. https://doi.org/10.1038/emi.2016.29.
Sharp, G.B., Kawaoka, Y., Wright, S.M., Turner, B., Hinshaw, V., Webster, R.G., 1993. Wild ducks are the reservoir for only a limited number of influenza a subtypes. Epidemiol. Infect. 110 (1), 161–176. https://doi.org/10.1017/S0950268800050780.
Suchard, M.A., Weiss, R.E., Sinsheimer, J.S., 2001. Bayesian selection of continuous-time Markov chain evolutionary models. Mol. Biol. Evol. 18 (6), 1001–1013. https://doi.org/10.1093/oxfordjournals.molbev.a003872. arXiv. http://oup/backfile/content_public/journal/mbe/18/6/10.1093_oxfordjournals.molbev.a003872/3/i0737-4038-018-06-1001.pdf.
Suchard, M.A., Lemey, P., Baele, G., Ayres, D.L., Drummond, A.J., Rambaut, A., 2018. Bayesian phylogenetic and phylodynamic data integration using beast 1.10. Virus Evol. 4 (1). https://doi.org/10.1093/ve/vey016. vey016. arXiv. http://oup/backfile/content_public/journal/ve/4/1/10.1093_ve_vey016/1/vey016.pdf.
Sun, Y., Liu, J., 2015. H9n2 influenza virus in China: a cause of concern. In: Protein & Cell.
Sun, Y., Pu, J., Jiang, Z., Guan, T., Xia, Y., Xu, Q., Liu, L., Ma, B., Tian, F., Brown, E., Liu, J., 2010. Genotypic evolution and antigenic drift of h9n2 influenza viruses in China from 1994 to 2008. Vet. Microbiol. 146 (3–4), 215–225.
Wan, H., Perez, D.R., 2007. Amino acid 226 in the hemagglutinin of h9n2 influenza viruses determines cell tropism and replication in human airway epithelial cells. J. Virol. 81 (10), 5181–5191. https://doi.org/10.1128/JVI.02827-06. arXiv. https://jvi.asm.org/content/81/10/5181.full.pdf. https://jvi.asm.org/content/81/10/5181.
Wei, K., Li, Y., 2018. Global genetic variation and transmission dynamics of h9n2 avian influenza virus. Transboundary Emerg. Dis. 65 (2), 504–517. https://doi.org/10.1111/tbed.12733. arXiv. https://onlinelibrary.wiley.com/doi/pdf/10.1111/tbed.12733. https://onlinelibrary.wiley.com/doi/abs/10.1111/tbed.12733.
Xu, K., Li, K.S., Smith, G.J.D., Li, J.W., Tai, H., Zhang, J.X., Webster, R., Peiris, J.S.M., Chen, H., fei Guan, Y., 2007. Evolution and molecular epidemiology of h9n2 influenza a viruses from quail in southern China, 2000 to 2005. J. Virol. 81 6, 2635–2645.
Xu, K., Ferreri, L.M., Rimondi, A., Olivera, V., Romano, M.C., del Valle Ferreyra, H., Rago, V., Uhart, M.M., Chen, H., Sutton, T., Pereda, A., Pérez, D.R., 2012. Isolation and characterization of an h9n2 influenza virus isolated in Argentina. Virus Res. 168, 1–2 41–7.
Yang, J., Müller, N.F., Bouckaert, R., Xu, B., Drummond, A.J., 2019. Bayesian phylodynamics of avian influenza a virus h9n2 in asia with time-dependent predictors of migration. PLoS Comput. Biol. 15 (8), 1–21. https://doi.org/10.1371/journal.pcbi.1007189. https://doi.org/10.1371/journal.pcbi.1007189.
Yu, G., Smith, D.K., Zhu, H., Guan, Y., Lam, T.T.-Y., 2017. ggtree: anr package for visualization and annotation of phylogenetic trees with their covariates and other associated data. Methods Ecol. Evol. 8 (1), 28–36. https://doi.org/10.1111/2041-210X.12628. https://besjournals.onlinelibrary.wiley.com/doi/abs/10.1111/2041-210X.12628.
Zhang, Z., Chen, B., Chen, W., 1994. The study of avian influenza: iithe incidence and serological survey of avian influenza. Chin. J. Vet. Med. 20, 6–7.